

# The stability of the $O(N)$ invariant fixed point in three dimensions

M. Caselle<sup>a\*</sup> and M. Hasenbusch<sup>b†</sup>

<sup>a</sup> *Dipartimento di Fisica Teorica dell'Università di Torino  
Istituto Nazionale di Fisica Nucleare, Sezione di Torino  
via P.Giuria 1, I-10125 Torino, Italy*

<sup>b</sup> *Humboldt Universität zu Berlin, Institut für Physik  
Invalidenstr. 110, D-10099 Berlin, Germany*

## Abstract

We study the stability of the  $O(N)$  fixed point in three dimensions under perturbations of the cubic type. We address this problem in the three cases  $N = 2, 3, 4$  by using finite size scaling techniques and high precision Monte Carlo simulations. It is well known that there is a critical value  $2 < N_c < 4$  below which the  $O(N)$  fixed point is stable and above which the cubic fixed point becomes the stable one. While we cannot exclude that  $N_c < 3$ , as recently claimed by Kleinert and collaborators, our analysis strongly suggests that  $N_c$  coincides with 3.

---

\*e-mail: caselle @to.infn.it

†e-mail: hasenbus@birke.physik.hu-berlin.de

# 1 Introduction

Quantum field theories with  $\phi^4$  type interactions are of importance in several physical contexts. In particular, they represent one of the most powerful tools in the study of critical phenomena [1]. Due to their simplicity they allow perturbative expansions up to rather large orders from which one can extract estimates for various critical quantities (critical indices and amplitude ratios) comparable in precision with those of the most advanced Monte Carlo simulations. In the simplest case the theory contains a single field  $\phi$  and describes the Ising universality class (for a recent comparison between field theoretic and Monte Carlo predictions in this case see for instance [2]).

When the field  $\phi$  has more than one component the situation becomes more complex and different quartic interaction terms can be defined. The simplest one has the form  $(\sum_{i=1}^N \phi_i^2)^2$ . It is  $O(N)$  symmetric and describes the  $O(N)$  universality class to which belongs, for instance, the isotropic  $N$ -component Heisenberg ferromagnet. Besides this term, the most interesting additional contribution is  $\sum_{i=1}^N \phi_i^4$  which breaks the  $O(N)$  symmetry but preserves the cubic invariance. The cubic subgroup of  $O(N)$  is composed of permutations and reflections of the  $N$  components of the field. Note that in the following "cubic" always refers to the symmetry and not to a third power. The importance of the cubic term is due to the fact that in a real crystal the crystalline structure gives rise to anisotropies which are mainly of the cubic type. Thus real crystals are better described by mixed actions in which both the  $O(N)$  and the cubic term are present.

Besides this phenomenological reason, this mixed model is also interesting in itself as it is a simple non-trivial QFT with different fixed points in competition among them. In fact, it is easy to see that in this model there are four possible fixed points: the trivial Gaussian one, the Ising one (which corresponds to the situation in which the  $N$  components  $\phi_i$  decouple), the  $O(N)$  symmetric and the cubic one (see fig.1). It was shown more than twenty years ago [3] that while the Gaussian and Ising fixed points are always unstable, the  $O(N)$  and cubic ones interchange their role as  $N$  increases. For  $N < N_c$  the  $O(N)$  symmetric point is stable, while for  $N > N_c$  it is destabilized by the cubic interaction and the cubic fixed point becomes the stable one (see fig.1). It is possible to see within the framework of the  $\epsilon$ -expansion that in three dimensions  $N_c < 4$ . The common lore, (supported by  $\epsilon$ -expansion up to the third order) has always been that  $N_c$  should lie somewhere between 3 and 4 in three dimensions, thus implying that the  $N = 3$  case, which is the most interesting one for applications to real crystals, should have a stable  $O(3)$  symmetric fixed point.

In these last years, this commonly accepted scenario has been contrasted in a series of papers [4, 5, 6, 7, 8] which suggested that  $N_c$  should lie *below* 3. As a consequence the critical behaviour of magnetic transitions in real crystals should be described by the cubic symmetric fixed point, a result which, if confirmed, would be of relevant interest from a theoretical point of view.

The aim of this paper is to test this conjecture with a high precision Monte Carlo simulation. By studying finite size corrections of a cubic invariant perturbation term exactly at the critical  $O(N)$  point we can extract the eigenvalues of the stability matrix of the  $O(N)$  fixed point. We study the three interesting cases  $N = 2, 3, 4$ . For  $N = 2$  and  $N = 4$  the expected results (stability of the isotropic and cubic fixed point respectively) are immediately visible from the data. In the  $N = 3$  case our results imply that  $N_c \approx 3$ . Obviously the numerical simulation can not decide whether  $N_c = 3$  is an exact result. However we obtain an upper bound for the absolute value of the stability index  $|b_2|$  for the  $O(3)$  fixed point, which turns out to be impressively small. In particular we are able to exclude all the existing estimates [4, 5, 9, 10, 11, 12] except that of Kleinert and collaborators [6, 7, 8], which is still compatible, within one standard deviation, with our result.

## 2 The cubic model

We are interested in the three dimensional quantum field theory defined by the Lagrangian

$$\mathcal{L} = \frac{1}{2} \sum_{i=1}^N (\partial_\mu \phi_i \partial^\mu \phi_i + m^2 \phi_i^2) + \frac{\lambda}{4!} (\sum_{i=1}^N \phi_i^2)^2 + \frac{\mu}{4!} \sum_{i=1}^N \phi_i^4 \quad . \quad (1)$$

While the term  $(\sum_{i=1}^N \phi_i^2)^2$  is  $O(N)$  symmetric, the term  $\sum_{i=1}^N \phi_i^4$  is only invariant under the “cubic” subgroup composed by permutations and reflections of the  $N$  components  $\phi_i$ . This model is discussed in great detail in several quantum field theory text books [1].

In the following we shall review the first order results in the  $\epsilon$ -expansion. This rather simple approximation already gives all the qualitative features of the renormalization flows of the model.

The fixed points of the theory are given by the zeros of the  $\beta$ -functions. The stability matrices are given by the derivatives of the  $\beta$ -functions at the zeros. From the eigenvalues of these matrices it is then easy to identify the stable fixed point.

The two  $\beta$ -functions are given, at the first order in the  $\epsilon$ -expansion, by

$$\beta_u = -\epsilon u + u^2 \frac{N+8}{6} + uv \quad (2)$$

$$\beta_v = -\epsilon v + \frac{3}{2} v^2 + 2uv \quad , \quad (3)$$

where  $u$  and  $v$  are the renormalized couplings related to  $\lambda$  and  $\mu$  respectively.

By looking at the zeros of the  $\beta$ -functions one sees that there are four possible fixed points:

- 1] The Gaussian fixed point  $u = 0, \quad v = 0$  .
- 2] The Ising fixed point  $u = 0, \quad v = \frac{2}{3}\epsilon$  .

3] The Heisenberg ( $O(N)$  invariant) fixed point  $u = \frac{6}{N+8}\epsilon$ ,  $v = 0$ .

4] The Cubic fixed point  $u = \frac{2}{N}\epsilon$ ,  $v = \frac{2(N-4)}{3N}\epsilon$ .

The stability matrix is defined as

$$B = \begin{pmatrix} \frac{\partial \beta_u(u,v)}{\partial u} & \frac{\partial \beta_u(u,v)}{\partial v} \\ \frac{\partial \beta_v(u,v)}{\partial u} & \frac{\partial \beta_v(u,v)}{\partial v} \end{pmatrix}. \quad (4)$$

At the first order of the  $\epsilon$ -expansion one obtains

$$B = \begin{pmatrix} -\epsilon + \frac{N+8}{3}u + v & u \\ 2v & -\epsilon + 2u + 3v \end{pmatrix}. \quad (5)$$

The corresponding eigenvalues, evaluated at the four fixed points are:

1] Gaussian :  $b_1 = b_2 = -\epsilon$ .

2] Ising :  $b_1 = -\frac{\epsilon}{3}$ ,  $b_2 = \epsilon$ .

3] Heisenberg :  $b_1 = \epsilon$ ,  $b_2 = \frac{4-N}{N+8}\epsilon$ .

4] Cubic fixed point:  $b_1 = N\epsilon$ ,  $b_2 = \frac{N-4}{3}\epsilon$ .

It is easy to see that the Gaussian and Ising fixed points are always unstable, independently from the value of  $N$ . In particular the Ising f.p. has only one direction of instability, while the Gaussian one is unstable in both directions.

The cubic and  $O(N)$  fixed points interchange their role as a function of  $N$ . For  $N$  smaller than a critical value  $N_c$  (which at this order in the  $\epsilon$ -expansion turns out to be 4) the Heisenberg fixed point is the stable one and defines the universality class toward which the system flows in the infrared limit.

For  $N > N_c$ ,  $b_2$  evaluated at the Heisenberg point becomes negative while  $b_2$  evaluated at the cubic f.p. becomes positive and the cubic fixed point becomes the stable one.

The renormalization flows corresponding to these two situations are reported in fig.1. For  $N < N_c$  all initial points with  $u > 0$  and  $v > \frac{N-4}{3}u$  will flow toward the  $O(N)$ -invariant, Heisenberg fixed point. For  $N > N_c$  all initial points with  $u > 0$  and  $v > 0$  will flow in the infrared limit toward the cubic fixed point which, for  $N < N_c$  lies in the  $v < 0$  half plane, exactly at  $N = N_c$  crosses the  $v = 0$  axis and moves for  $N > N_c$  in the  $v > 0$  region.

Initial points outside the above defined regions flow away toward more negative values of  $u$  and/or  $v$  and finally reach the region in which the positivity condition for the quartic potential is no longer satisfied. These trajectories are related (from the statistical mechanics point of view) to realizations of the cubic model in which the phase transition is of the fluctuation-induced first order type. These models

have recently attracted much interest as a laboratory to study arbitrary weak first order transitions [13].

The last remaining point is now to find the value of  $N_c$  in three dimensions. It is easy to see by looking to higher orders in the  $\epsilon$ -expansion, or with the help of Monte Carlo simulations, that for  $N = 2$  the Heisenberg fixed point is stable and that on the contrary for  $N = 4$  the cubic fixed point is the stable one. Thus  $2 < N_c < 4$ . However it turns out to be hard to decide whether  $N_c$  is greater or lower than 3. Equivalently one can look at the sign of the  $b_2$  eigenvalue at the Heisenberg point for  $N = 3$ . If  $b_2$  is positive, then  $N_c$  must be greater than 3. In the past twenty years much efforts have been devoted to settle this question. The first result was reported in [9] where the  $\epsilon$ -expansion for  $N_c$  was extended up to the third order leading to the estimate  $N_c = 3.128$ . In agreement with this estimate (but, using a completely different approach), Grover, Kadanoff and Wegner [10] obtained  $b_2 = 0.053$  at  $N = 3$ . Few years later, with different approximation techniques, the two contrasting results:  $N_c \sim 2.3$  [11] and  $N_c \sim 3.4$  [12] were obtained. Ten years later in [4, 5] a value  $N_c < 3$  was suggested. In particular in [5], by means of a three loop calculation directly in  $d = 3$ , the values  $N_c = 2.91$  and  $b_2 = -0.008$  were proposed. Finally, more recently, Kleinert and collaborators pushed the  $\epsilon$ -expansion up to the fifth order [7] and obtained a similar answer. First, in [7] they found, (with a [2,2] Pade' approximant)  $N_c = 2.958$ . Then in [8], by using a careful resummation procedure of the fifth order series, they obtained the value  $b_2 = -0.00214$  for the stability eigenvalue at  $N = 3$ . Due to the nature of these results it is very difficult to add sensible error-bars to these estimates. However, it is clear from the above discussion that the existing estimates for  $N_c$  are scattered around  $N_c = 3$  and that as the various techniques and approximations become more and more refined the corresponding estimates for  $N_c$  get closer and closer to  $N_c = 3$ .

## 3 The simulation

### 3.1 The model

The cubic model discussed in sect.2 has a simple and straightforward lattice realization, defined by the action:

$$S = -\beta \sum_{\langle xy \rangle} s_x s_y - \mu \sum_x \sum_{i=1}^N (s_x^i)^4, \quad (6)$$

where  $s_x$  is a unit vector in  $R^N$ .  $\langle x, y \rangle$  denotes a pair of nearest neighbour sites on the lattice. We consider a three-dimensional cubic lattice of size  $L$  and lattice spacing  $a = 1$ . For  $\mu = 0$  we have the standard  $O(N)$  invariant (Heisenberg) model, while for  $\mu \neq 0$  the cubic-invariant perturbation  $\sum_x \sum_{i=1}^N (s_x^i)^4$  breaks the  $O(N)$  symmetry. In the following we shall study this model in the three cases  $N = 2, 3, 4$ . We shall concentrate our main efforts in the  $N = 3$  case.

In three dimensions, for  $\mu = 0$ , the  $O(N)$  model undergoes a second order phase transition for some value  $\beta_c$  (which depends on  $N$ ) of the coupling. In the vicinity of such a point the continuum limit can be taken, leading to the  $O(N)$  symmetric QFT (corresponding to the  $v = 0$  axis in fig.1) discussed in the previous section. The presence of such a continuous phase transition is obviously a mandatory condition for the whole analysis.

The simplest way to extract the value of  $N_c$  from a lattice simulation is to determine the stability eigenvalues  $b_2$  for  $N = 3$ . From the lattice point of view the  $b_2$  eigenvalue appears as the critical index which controls the behaviour of any cubic-invariant (but  $O(N)$ -violating) observable in the vicinity of the Heisenberg transition point.

The most efficient way to evaluate such a critical index is to look at the finite size dependence (as a function of the lattice size  $L$ ) of a suitable observable (to be defined below) evaluated exactly at the critical point  $\beta_c$ . To this end it is necessary to have a very good estimate of the critical coupling. Fortunately,  $\beta_c$  is known with very high precision in each of the three cases  $N = 2, 3, 4$  in which we are interested. This is one of the reasons for which we have chosen this particular lattice realization of the cubic model.

In tab.1,2,3 we have collected the most recent results for  $\beta_c$  both from Monte Carlo simulations and from series expansions. HT- $\theta$  indicates the biased resummation of the HT series in which the value of the index  $\theta$  is given as input parameter. It is interesting to see that all the estimates agree within the errors.

In tab.4 we report the values (chosen from tab.1,2,3) that we used in our simulations.

Table 1: *Results for  $\beta_c$  given in the literature for  $N = 2$*

ref.	method	$\beta_c$
[14]	MCRG	0.45420(2)
[14]	MC	0.454170(7)
[15]	MC	0.454165(4)
[16]	HT	0.45419(3)

Table 2: *Results for  $\beta_c$  given in the literature for  $N = 3$*

ref.	method	$\beta_c$
[17]	MC	0.6930(1)
[18]	MC	0.6931(1)
[19]	MC	0.693035(37)
[15]	MC	0.693002(12)
[16]	HT	0.69303(3)
[16]	HT- $\theta$	0.69305(4)

Table 3: Results for  $\beta_c$  given in the literature for  $N = 4$

ref.	method	$\beta_c$
[20]	MC	0.9360(1)
[15]	MC	0.935861(8)
[16]	HT	0.93589(6)
[16]	HT- $\theta$	0.93593(6)

Table 4: Values of  $\beta_c$  used in this article.

N	$\beta_c$
2	0.454165(4)
3	0.693002(12)
4	0.935861(8)

### 3.2 Observables

There are four natural observables in the model (6). The two terms which appear in the action:

$$E \equiv \sum_{\langle xy \rangle} s_x s_y \quad (7)$$

and

$$P \equiv \sum_x \sum_i (s_x^i)^4 \quad (8)$$

The total magnetization, which is the order parameter of the transition:

$$M \equiv \sum_x s_x \quad (9)$$

and the ratio

$$R = \frac{\sum_i (M^i)^4}{(M^2)^2} \quad (10)$$

which quantifies the violation of the  $O(N)$  symmetry in the model <sup>1</sup>.

In order to study the stability of the fixed point we are actually interested in the derivative of  $\langle R \rangle$  with respect to  $\mu$  at  $\beta = \beta_c$  and  $\mu = 0$ :

$$D_R \equiv \left. \frac{\partial \langle R \rangle}{\partial \mu} \right|_{\mu=0, \beta=\beta_c} \quad (12)$$

---

<sup>1</sup>Other choices are possible for this last observable. For instance the term

$$X = \frac{M_{max}^2}{M^2} \quad (11)$$

where  $M_{max}^2$  is the maximal square of a component of the magnetization would work equally well. However it turns out that the ratio  $R$  defined above is the one which can be measured in the most efficient and simple way.

In fact this derivative measures the (generalized) susceptibility of the system with respect to a cubic perturbation, just like what happens for the ordinary magnetic susceptibility in the case of a magnetic perturbation or for the specific heat in the case of a thermal perturbation. At this point, a standard finite size scaling analysis tells us that the critical index which measures the infrared stability of the system with respect to the above perturbations, also controls the finite size behaviour (namely the  $L$  dependence) of the corresponding susceptibility exactly at the critical point. In particular, in the case in which we are interested,  $D_R$  should behave for  $\beta = \beta_c$  and  $\mu = 0$ , as

$$D_R \propto L^{-b_2} \quad . \quad (13)$$

where  $b_2$  is exactly the stability eigenvalue of the Heisenberg fixed point that we are looking for.

Scaling laws of the type (13) are expected to hold for sufficiently large values of  $L$ . For small lattices, correction to scaling terms should be expected. It is thus important to have results with small statistical errors for large lattice sizes. Few preliminary tests have shown us that (at least for the case  $N = 3$ ) sizes up to  $L = 32$  are needed to extract reliable estimates of  $b_2$ . This requirement represents the major technical problem of this work.

There are two possible choices to compute  $D_R$ :

- It can be computed directly in the simulation at  $\mu = 0$  as

$$D_R = \langle PR \rangle - \langle P \rangle \langle R \rangle \quad . \quad (14)$$

- It can be computed by using the finite difference method, i.e. by simulating the model at small non-zero values of  $\mu$ :

$$D_R(\mu) \equiv \frac{R(\mu) - R(-\mu)}{2\mu} \quad . \quad (15)$$

It is easy to recover the relationship between  $D_R$  and  $D_R(\mu)$ . First, let us notice that on a finite lattice  $R(\mu, \beta)$  must be an analytic function of its parameters. This holds also at  $\beta = \beta_c$ . Therefore we can Taylor-expand  $R(\mu, \beta)$  in powers of  $\mu$  for fixed  $\beta = \beta_c$ . Taking the symmetric difference we obtain

$$D_R = D_R(\mu) + \frac{1}{3!} \frac{d^3 R}{d\mu^3} \mu^2 + O(\mu^4) \quad . \quad (16)$$

Both these definitions have their drawbacks. The  $\mu = 0$  simulations are affected by a strong enhancement of the variance (hence of the statistical errors) as  $L$  increases. It turns out that the statistical error of  $D_R$  at a fixed number of measurements increases roughly as  $L^{3/2}$ . As a consequence too large samples are needed to keep the error sufficiently small for  $L > 16$ .



On the contrary for  $D_R(\mu)$  at fixed  $\mu$  the statistical error does not increase with  $L$ . However the  $O(\mu^2)$  corrections do increase with  $L$ . Reducing these  $O(\mu^2)$  corrections requires to reduce the value of  $\mu$ . This in turn requires to increase the number of measurements to keep the statistical error fixed.

In the following section we shall discuss a way out of these problems. By using the global  $O(N)$  symmetry of the model at  $\mu = 0$  an improved version of  $D_R$  can be constructed. This improvement does not change the  $L$  dependence of the variance, but gives a significant reduction of its magnitude, thus allowing to reach, with a reasonable CPU time, lattices sizes as large as  $L = 32$  which are large enough to extract the finite size behaviour with the required precision. Most of the data that we shall discuss in the last section have been obtained by using this improved observable. We also performed, as a cross check, some simulations at finite  $\mu$ . The agreement that we find between the values of  $D_R$  obtained in these two ways is a non trivial check of the reliability of our results.

### 3.3 Variance reduced estimator for $D_R$ .

Variance reduced estimators have the same expectation value as the corresponding standard estimators. However their variance is reduced, which allows for more accurate results in Monte Carlo simulations than the standard estimator. A general principle to construct variance reduced estimators is to look for degrees of freedom which can be integrated out analytically.

In order to obtain a variance reduced estimator of  $\frac{\partial \langle R \rangle}{\partial \mu}$  we integrate  $P, R$  and  $PR$  over the global  $O(N)$  rotations.

This is trivial for  $P$  and  $R$ , but it is less simple in the case of the  $PR$  component. Since  $P$  is a sum over all lattice sites we can commute the integration over the global rotations and the summation over the lattice sites. The integral to be solved is hence given by

$$I = \int_{O(N)} DT \left( \sum_i [(Ts_x)^i]^4 \right) \left( \sum_i [(Tm)^i]^4 \right) , \quad (17)$$

where  $T$  is an element of  $O(N)$ ,  $DT$  the Haar-measure,  $s_x$  the spin at the site  $x$ , and  $m$  a unit vector in the direction of the global magnetization. For symmetry reasons the integral only depends on the angle between  $s_x$  and  $m$ , which we define as follows:

$$ms_x = \cos(\alpha) \quad . \quad (18)$$

The integral (17) can be evaluated explicitly for any value of  $N$ . Details of the calculation are reported in the appendix. Here we only list the results in the three cases in which we are interested:

$$N = 2$$

$$I = \frac{9}{16} + \frac{1}{32} \cos(4\alpha) \quad (19)$$

$N = 3$

$$I = \frac{1}{60} \cos(4\alpha) + \frac{1}{105} \cos(2\alpha) + \frac{153}{420} \quad (20)$$

$N = 4$

$$I = \frac{2}{25} \cos^4(\alpha) - \frac{3}{50} \cos^2(\alpha) + \frac{51}{200} \quad (21)$$

### 3.4 The Monte Carlo Algorithm

Due to the different symmetries in the models, we had to use different algorithms in the two cases  $\mu = 0$  and  $\mu \neq 0$ .

#### 3.4.1 $\mu = 0$

In the case  $\mu = 0$  we used the single cluster algorithm of U.Wolff [21] and the microcanonical overrelaxation algorithm. The basic idea of the cluster-algorithm is to construct conditional Ising models. This is achieved by allowing only the sign-change of the spin component parallel to an unit vector  $r$  in  $R^N$ . The delete probability depends on the pair of lattice sites and is given by

$$p_d(x, y) = \min[1, \exp(-2(rs_x)(rs_y))] \quad , \quad (22)$$

where  $x$  and  $y$  are nearest neighbour sites on the lattice. The vector  $r$  is chosen with a probability density uniform on  $S^{N-1}$ . For each update a new  $r$  is chosen.

The variance of the improved estimator of  $D_R$  is mainly caused by local fluctuations of the spins. Hence it is useful to supplement the cluster-algorithm with a fast local algorithm to produce local changes of the configuration. For that purpose we used the microcanonical overrelaxation algorithm.

The elementary update of the algorithm is given by

$$s'_x = \frac{2 (n_x s_x) n_x}{n_x^2} - s_x \quad , \quad (23)$$

where  $n_x$  is the sum of the nearest neighbour spins of  $s_x$ . Since neither a random number nor the evaluation of the exponential function is needed for this update the CPU-time required is rather small compared with a Metropolis or a heat-bath update.

The whole update cycle that we used in our simulations consists of a mixture of 9 overrelaxation sweeps and  $K$  cluster-updates.  $K$  is chosen such that the number of spins updated in  $K$  cluster-updates is of the order of the number of lattice-sites. A measurement is performed after each overrelaxation sweeps and after the cluster-updates. There are hence 10 measurements in the 9 overrelaxation sweeps and  $K$  cluster-updates cycle.

### 3.4.2 $\mu \neq 0$

For  $\mu \neq 0$  some modifications are needed. We have restricted the vector  $r$  such that  $\sum_i (s^i)^4$  is not changed by the update. This is guaranteed if the sign of a component is changed or two components are exchanged or a combination of both. This means that  $r$  is either parallel to an axis or is diagonal in a plane.

$r$  is in

$$(1, 0, \dots, 0), (0, 1, \dots, 0) \dots (0, 0, \dots, 1) \quad (24)$$

or

$$\frac{1}{\sqrt{2}}(1, 1, \dots, 0), \frac{1}{\sqrt{2}}(1, 0, \dots, 1), \dots \frac{1}{\sqrt{2}}(0, \dots, 1, 1) \quad (25)$$

or

$$\frac{1}{\sqrt{2}}(1, -1, \dots, 0), \frac{1}{\sqrt{2}}(1, 0, \dots, -1), \dots \frac{1}{\sqrt{2}}(0, \dots, 1, -1) \quad (26)$$

While this restriction of  $r$  to a discrete subset of  $S^{N-1}$  does not violate detailed balance it means that the cluster-update by itself is not ergodic.

In order to restore ergodicity we supplement the cluster-update with an (ergodic) Metropolis update. For performance reasons we also added a local reflection update that is microcanonical for  $\mu = 0$ . A spin is reflected at the sum of its neighbours.

$$s'_x = \frac{(S_x s_x) S_x}{S_x^2} - 2s_x \quad (27)$$

where  $S_x$  is the sum of the spins on nearest neighbour sites of  $x$ . For  $\mu \neq 0$  the proposal  $s'_x$  is accepted with a probability

$$P_{acc} = \min[1, \exp(\mu \sum_i [(s_x^i)^4 - (s_x^i)^4])] \quad (28)$$

A whole update cycle consists of one Metropolis update, one local reflection update plus  $K$  cluster-updates.  $K$  is chosen, as in the  $\mu = 0$ , case such that the number of spins updated in  $K$  cluster-updates is of the order of the number of lattice-sites. A measure is performed in each update cycle.

## 3.5 Statistical and systematic errors

We evaluated statistical errors with the standard binning method. Both in the  $\mu = 0$  and  $\mu \neq 0$  cases bins of 1.000 update cycles are chosen (corresponding to 10.000 and 1.000 measurements respectively). This binning was already performed during the simulation since not all individual measurements could be stored on disc. Besides the statistical uncertainty we have to face also the systematic error due to the uncertainty  $\Delta\beta_c$  in the estimate of  $\beta_c$ . To evaluate this error we also measured in the simulation the expectation value  $\langle ER \rangle$ . The difference

$$\langle ER \rangle - \langle E \rangle \langle R \rangle \quad (29)$$

gives an estimate of the derivative of  $\langle R \rangle$  with respect to  $\beta$ , from which we can obtain the systematic error induced on  $R$  by the uncertainty in  $\beta_c$ :

$$(\langle ER \rangle - \langle E \rangle \langle R \rangle) * \Delta\beta_c . \quad (30)$$

With a similar construction we obtain the error induced on  $D_R$ . We can consider this as a lower bound on the accuracy that we can reach for the derivatives. It makes no sense to reduce the statistical error of  $D_R$  below this bound. This observation fixes the typical sample size for the simulations, which turned out to be of the order of 20.000 bins.

## 4 Results and discussion

### 4.1 Results at $\mu = 0$

We simulated the models with  $N = 2, 3, 4$  at  $\mu = 0$ ,  $\beta = \beta_c$ , in the ranges  $L \in [4 - 16]$  for  $N = 2$ ;  $L \in [4 - 32]$  for  $N = 3$  and  $L \in [4 - 20]$  for  $N = 4$ . The results are reported in tables 5, 6 and 7. In the first column we report the lattice size and in the second the values of the derivative  $D_R$ . the first error in parenthesis denotes the statistical uncertainty, while in the second parenthesis the error induced by the uncertainty in  $\beta_c$  is reported. In the last column we report the sample size (number of bins times number of measurements in each bin).

Table 5: *Results for  $D_R$  in the  $N = 2$  model*

L	$D_R$	statistics
4	.011046(20)(1)	10000 * $10^4$
6	.010506(34)(2)	10000 * $10^4$
8	.010121(51)(2)	10000 * $10^4$
10	.009728(58)(4)	15000 * $10^4$
12	.009523(76)(5)	15000 * $10^4$
16	.008904(117)(4)	15000 * $10^4$

### 4.2 Results at $\mu \neq 0$

As a test of the above results we also performed some simulations at  $\mu \neq 0$ , both for  $N = 2$  and  $N = 3$ . We evaluated the finite  $\mu$  estimators  $D_R(\mu)$  by using eq.(15). The results are reported in tab.8 where, in the last line, we also reported for comparison the corresponding  $\mu = 0$  estimates.

The agreement between the results obtained with the two approaches is very good and makes us confident on the reliability of the  $\mu = 0$  set of data.

Table 6: *Results for  $D_R$  in the  $N = 3$  model*

L	$D_R$	statistics
4	.019672(19)(3)	$10000 * 10^4$
6	.020118(19)(5)	$15000 * 10^4$
8	.020187(20)(7)	$20004 * 10^4$
10	.020196(25)(10)	$20870 * 10^4$
12	.020152(32)(13)	$21500 * 10^4$
14	.020178(40)(15)	$20770 * 10^4$
16	.020233(49)(16)	$20750 * 10^4$
20	.020094(68)(22)	$20150 * 10^4$
24	.020178(84)(28)	$23145 * 10^4$
32	.020265(140)(39)	$19560 * 10^4$

Table 7: *Results for  $D_R$  in the  $N = 4$  model*

L	$D_R$	statistics
4	.023474(15)(1)	$10000 * 10^4$
6	.025287(16)(3)	$10000 * 10^4$
8	.026294(19)(4)	$10000 * 10^4$
10	.027097(23)(6)	$10000 * 10^4$
12	.027742(27)(8)	$10600 * 10^4$
16	.028774(39)(13)	$10000 * 10^4$
20	.029605(52)(38)	$10050 * 10^4$

### 4.3 The $b_2$ index

We fitted the data obtained at  $\mu = 0$  with the scaling law

$$D_R = C L^{-b_2} . \quad (31)$$

The fit results are collected in tab.9 where in the second column we give the minimum value  $L_{min}$  of  $L$  taken into account in the fit. In the third and fourth column we report the reduced  $\chi^2$  and the confidence level respectively. Finally, in the last two column the best fit values of  $C$  and  $b_2$  are reported. As usual we give in the first parenthesis the statistical error and in the second the error induced by  $\beta_c$ . The various fits are plotted and compared in fig.2 and 3.

The large value of  $\chi^2$  clearly indicates that for any value of  $N$  the sample at  $L = 4$  is strongly affected by correction to scaling terms and must be discarded. Fits without  $L = 4$  have an acceptable  $\chi^2$ . However this fact does not necessarily imply that it is justified to ignore corrections to scaling. Hence we regard the fits with  $L_{min} = 8$  as our final result. Still it remains difficult to quantify the systematic error due to corrections to scaling. Based on the experience with the finite size scaling analysis of other exponents of the Heisenberg model we expect them to be

Table 8: *Results for  $D_R$  for  $\mu \neq 0$*

	$N = 2, L = 8$	$N = 2, L = 12$	$N = 2, L = 16$	$N = 3, L = 12$
$\mu = 4$		.010503(140)(3)		
$\mu = 2$	.010117(28)(1)	.010008(122)(3)		
$\mu = 1$	.010112(57)(1)	.009495(118)(3)		.020977(64)(9)
$\mu = 0.5$	.010054(74)(1)	.009505(103)(3)	.009139(103)(4)	.020306(130)(9)
$\mu = 0.25$				.020076(257)(9)
$\mu = 0$	.010121(51)(2)	.009523(76)(5)	.008904(117)(4)	.020152(32)(13)

of the same order of magnitude as the statistical error of the  $L_{min} = 8$  fits.

Table 9: *Results for  $C$  and  $b_2$*

$N$	$L_{min}$	$\chi_{red}^2$	C.L.	$C$	$b_2$
2	4	2.01	9%	0.01335(9)(1)	0.1362(40)(3)
2	6	1.17	32%	0.01381(24)(1)	0.1519(84)(4)
2	8	0.85	43%	0.01445(54)(2)	0.1711(166)(6)
3	4	26.5	0%	0.01936(4)(2)	-0.0174(10)(6)
3	6	1.32	23%	0.02005(6)(2)	-0.0026(14)(7)
3	8	0.71	64%	0.02022(10)(3)	0.0007(20)(9)
4	4	77.5	0%	0.01928(3)(1)	-0.1473(7)(4)
4	6	1.22	30%	0.01997(5)(2)	-0.1321(10)(5)
4	8	0.51	67%	0.02008(8)(3)	-0.1299(16)(8)

#### 4.4 Discussion and comparison with other estimates

As it can be seen from tab.9, our results for  $N = 3$  are certainly incompatible with all the existing estimates [4, 5, 9, 10, 11, 12], except that of Kleinert and collaborators [6, 7, 8]. As a matter of fact, if we keep in the fit for  $N = 3$  also the  $L = 6$  sample we find an impressive agreement with the result  $b_2 = -0.00214$  of ref. [7]. However, as mentioned above, we strongly suspect that the  $L = 6$  sample is still affected by correction to scaling terms and prefer to quote as our best estimate the  $L = [8 - 32]$  result  $b_2 = 0.0007(20)(9)$ , which is still compatible with the result of ref. [7], but suggests that  $N_c$  could indeed exactly coincide with 3. In this respect it must also be noticed that the trend of the perturbative estimates of  $b_2$  quoted in [7] as a function of the order in the perturbative expansion also suggests that  $N_c$  converges to 3 in agreement with our result.

In any case, let us stress again that it is obviously impossible to decide by means of a numerical simulation if  $N_c = 3$  is an exact result and that the fact that the difference  $|N_c - 3|$  is so small, and compatible with zero, might well be a coincidence. However we think that it would be worthwhile to look for an argument

which explains why the cubic and Heisenberg fixed point in three dimensions should coincide exactly for  $N=3$ .

### **Acknowledgements**

We thank F.Gliozzi, G.Münster, K.Pinn, P.Provero and S.Vinti for many helpful discussions. Work supported in part by the European Commission TMR programme ERBFMRX-CT96-0045.

## Appendix

In this appendix we evaluate the integral

$$I = \int_{O(N)} DT \left( \sum_i [(Ts_x)^i]^4 \right) \left( \sum_i [(Tm)^i]^4 \right) , \quad (\text{A.1})$$

where  $T$  is an element of  $O(N)$ ,  $DT$  the Haar-measure,  $s_x$  the spin at the site  $x$  and  $m$  a unit vector in the direction of the global magnetization. For symmetry reasons the integral only depends on the angle between  $s_x$  and  $m$  which is defined as

$$ms_x = \cos(\alpha) . \quad (\text{A.2})$$

We write the integral as

$$I(\alpha) = \int_{S^{N-1}} ds \left( \sum_i s_i^4 \right) \int_{S^{N-2},s} dt \left( \sum_i t_i^4 \right) , \quad (\text{A.3})$$

where  $\int_{S^{N-1}}$  denotes the integral over the  $N$  dimensional sphere.  $\int_{S^{N-2},s}$  denotes the integral over the  $N-1$  dimensional subspace defined as the set of all the vectors  $t$  that for any fixed  $s$  satisfy the equation  $st = \cos(\alpha)$ . We choose the normalizations so that  $\int_{S^{N-1}} ds = 1$  and  $\int_{S^{N-2},s} dt = 1$

Because of symmetry we can restrict the calculation to the first component of  $s$

$$I(\alpha) = N \int_{S^{N-1}} ds s_1^4 \int_{S^{N-2},s} dt \left( \sum_i t_i^4 \right) . \quad (\text{A.4})$$

Now we decompose the integral  $\int_{S^{N-1}}$  into the integral over the  $s_1$  component and for fixed  $s_1$  over the remaining  $S^{N-2}$ .

We get

$$I(\alpha) = N \text{ const} \int_{s_1=0}^{s_1=1} ds_1 (1 - s_1^2)^{(N-3)/2} s_1^4 \int_{S^{N-2}} ds' \int_{S^{N-2},s} dt \left( \sum_i t_i^4 \right) , \quad (\text{A.5})$$

where

$$\text{const}_1 = \left[ \int_{s_1=0}^{s_1=1} ds_1 (1 - s_1^2)^{(N-3)/2} \right]^{-1} \quad (\text{A.6})$$

and  $s'$  is  $s$  without the 1-component.

Let us now study

$$\int_{S^{N-2}} ds' \int_{S^{N-2},s} dt . \quad (\text{A.7})$$

This measure for  $t$  is invariant under rotations around the 1-axis. The non-trivial question is the measure for the 1-component of  $t$ . The range of  $t_1$  is given by

$$t_{max} = \cos(\alpha)s_1 + \sin(\alpha)\sqrt{1 - s_1^2} \quad (\text{A.8})$$



and

$$t_{min} = \cos(\alpha)s_1 - \sin(\alpha)\sqrt{1 - s_1^2} . \quad (\text{A.9})$$

The measure between this extreme values is given by the fact that for any  $s, t$  is distributed on a  $S^{N-2}$  sphere. Hence the measure is (for  $N > 2$ )

$$const_2 \left[ 1 - \left( \frac{t_1 - c}{2s} \right)^2 \right]^{(N-4)/2} \quad (\text{A.10})$$

with  $c = \cos(\alpha)s_1$  and  $s = \sin(\alpha)\sqrt{1 - s_1^2}$ . The normalization  $const_2$  is given by

$$const_2 = \left\{ \int_{t_1=c-s}^{c+s} \left[ 1 - \left( \frac{t_1 - c}{2s} \right)^2 \right]^{(N-4)/2} dt_1 \right\}^{-1} . \quad (\text{A.11})$$

For fixed  $t_1$  the integration of the remaining components gives us  $(1 - t_1^2)^2 < R >_{N-1}$ , with  $< R >_N = 3/(N+2)$ .

Now we are in the position to write down the full integral:

$$I(\alpha) = N \, const_1 \int_{s_1=0}^{s_1=1} ds_1 (1 - s_1^2)^{(N-3)/2} s_1^4 \quad (\text{A.12})$$

$$const_2 \int_{t_1=c-s}^{c+s} \left[ 1 - \left( \frac{t_1 - c}{2s} \right)^2 \right]^{(N-4)/2} (t_1^4 + \frac{3}{N+1}(1 - t_1^2)^2) . \quad (\text{A.13})$$

This integral can be solved with standard techniques and yields in the three cases  $N = 2, 3, 4$  the results listed in sect. 3

## Figure Captions

**Fig.1** Renormalization group flows for the cubic model in three dimensions.

**Fig.2**  $\text{Log}(D_R)$  as a function of  $\text{Log}(L)$ . Triangles squares and circles denote the  $N = 4$ ,  $N = 3$  and  $N = 2$  data respectively. Errors are not reported since they are smaller than the symbol sizes. To render easier the comparison among the three sets of data, all the values of  $D_R$  have been normalized to the best fit value of the constant  $C$  (see tab.9 for the value of  $C$ ). The three lines correspond to the best fits obtained neglecting the  $L = 6$  derivative.

**Fig.3** The  $N = 3$  data only, plotted with a much higher resolution. The dotted line corresponds to the best fit *including*  $L = 6$ , while the dashed line corresponds to the  $L = [8 - 32]$  fit. All the points are normalized as in fig.2.

## References

- [1] See for instance: D.J.Amit, *Field Theory, the Renormalization Group and Critical Phenomena*, World Scientific, Second Edition (1989);  
J. Zinn-Justin, *Quantum Field Theory and Critical Phenomena*, Clarendon Press, Oxford, Third Edition (1996).
- [2] M.Caselle and M.Hasenbusch, J. Phys. **A30** (1997) 4963.
- [3] A.Aharony, Phys. Rev. **B8** (1973) 4270.
- [4] I.O. Mayer and A.I. Sokolov, Izv. Akad. Nauk SSSR Ser. Fiz. **51** (1987) 2103,  
I.O. Mayer, A.I. Sokolov, and B. N. Shalayeve, Ferroelectrics **95** (1989) 93.
- [5] N.A. Shpot, Phys. Lett. **A142** (1989) 474.
- [6] H.Kleinert and S. Thoms, Phys. Rev. **D52** (1995) 5926.
- [7] H.Kleinert and V. Schulte-Frohlinde, Phys. Lett. **B342** (1995) 284.
- [8] H.Kleinert, S. Thoms and V. Schulte-Frohlinde, preprint quant-ph/9611050.
- [9] I.J. Ketley and D.J. Wallace, J. Phys. **A6** (1973) 1667.  
D.R.Nelson, J.M.Kosterlitz and M.E.Fisher, Phys. Rev. Lett. **33** (1974) 813.
- [10] M.K. Grover, L.P. Kadanoff and F.J. Wegner Phys. Rev. **B6** (1972) 311.
- [11] M.C.Yalabik and A. Houghton, Phys. Lett. **61A** (1977) 1.
- [12] K.E. Newman and E.K. Riedel, Phys. Rev. **B25** (1982) 264.

- [13] See for instance: N. Tetradis, hep-th/9706088 and references therein.
- [14] A.Gottlob and M.Hasenbusch, Physica **A201** (1993) 593
- [15] H.G.Ballestreros, L.A. Fernandez, V. Martin-Mayor and A. Munoz Sudupe, Phys. Lett. **B387** (1996) 125
- [16] P.Butera and M.Comi, hep-lat/9703018
- [17] C.Holm and W.Janke, hep-lat 9301002, Phys.Rev. **B48** (1993) 936.
- [18] R.G.Brown and M.Ciftan. Phys. Rev. Lett. **76** (1996) 1352.
- [19] K.Chen, A.M.Ferrenberg and D.P.Landau, Phys. Rev. **B48** (1993) 3249
- [20] K.Kanaya and S.Kaya, Phys. Rev. **D51** (1995) 2404
- [21] U. Wolff, Phys. Rev. Lett. **62** (1989) 361.

**Fig. 1**

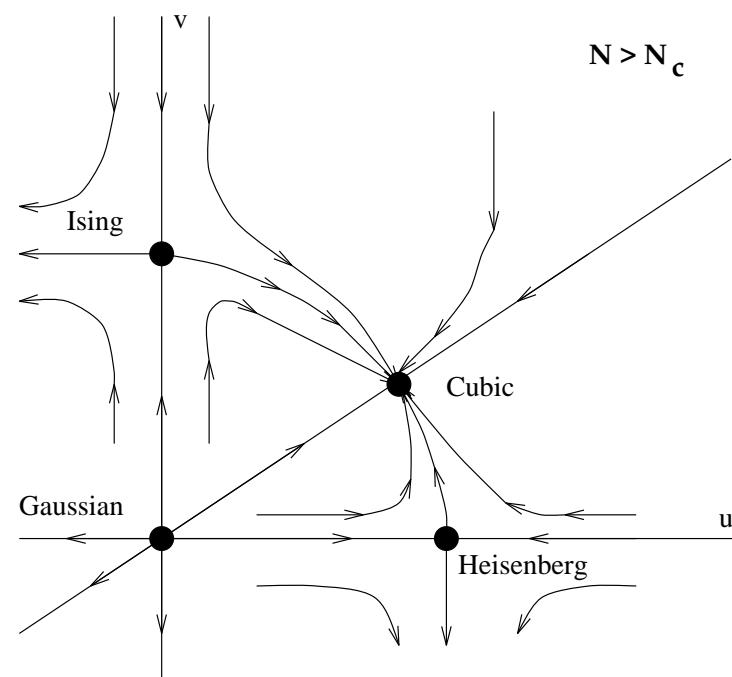
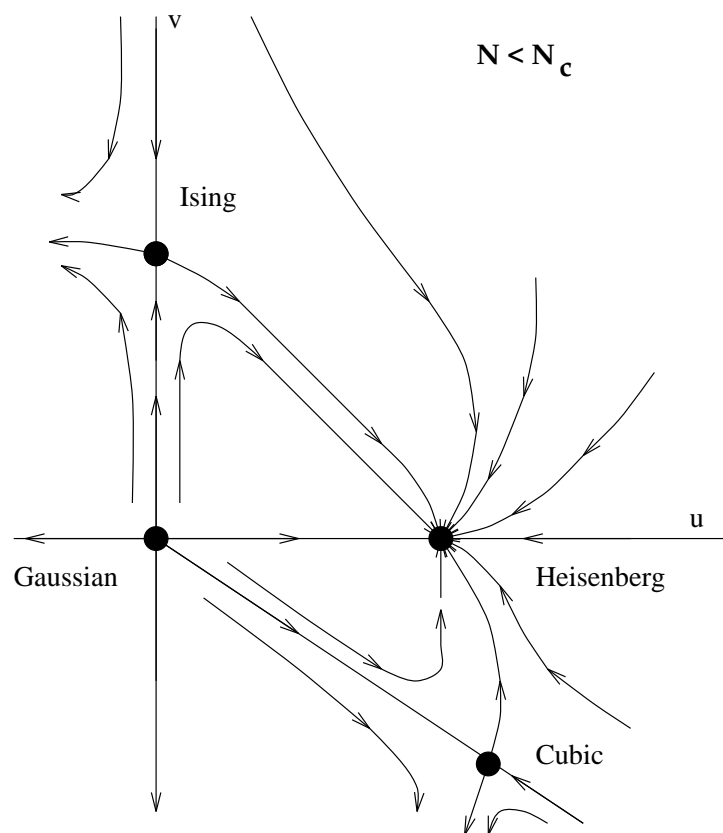


Fig. 2

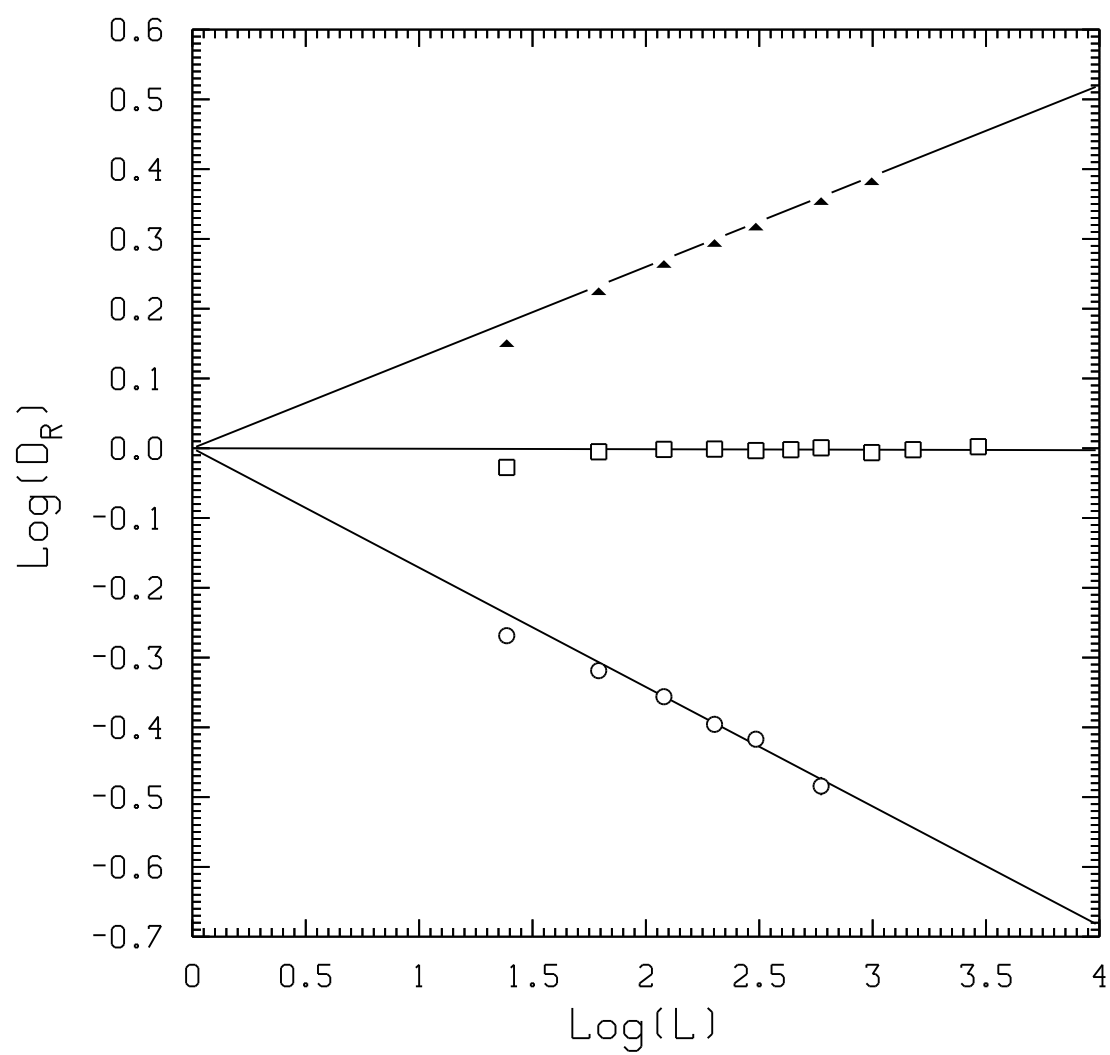


Fig. 3

